



A Multidisciplinary Optimization Using Semi-Analytical Sensitivity Analysis Procedure and Multilevel Decomposition

A. CHATTOPADHYAY AND N. PAGALDIPTI

Department of Mechanical and Aerospace Engineering
Arizona State University, Tempe, AZ 85287-6106, U.S.A.

(Received February 1994; revised and accepted July 1994)

Abstract—This paper addresses the development of a multidisciplinary optimization procedure using an efficient semi-analytical sensitivity analysis technique and multilevel decomposition for the design of aerospace vehicles. A semi-analytical sensitivity analysis procedure is developed for aerodynamic design sensitivities. Accuracy and efficiency of the sensitivity analysis procedure is established through comparison of the results with those obtained using a finite difference technique. The optimization problem, with the integration of aerodynamics and structures, is decomposed into two levels. Optimization is performed for improved aerodynamic performance at the first level and improved structural performance at the second level. Aerodynamic analysis is performed by solving the three-dimensional parabolized Navier Stokes equations. A nonlinear programming technique and an approximate analysis procedure are used for optimization. The procedure developed is applied to design the wing of a high speed aircraft. Results obtained show significant improvements in the wing aerodynamic and structural performance when compared to a reference or baseline wing configuration. The use of the semi-analytical sensitivity technique provides significant computational savings.

Keywords—Optimization, Semi-analytical, Sensitivity analysis, Multidisciplinary, Multilevel decomposition, Computational fluid dynamics.

NOMENCLATURE

c_0	wing root chord	C_D	drag coefficient
g	constraint functions	C_L	lift coefficient
p_i	parameter used in approximate analysis	D	drag
t_c	wing thickness to chord ratio	F	objective function vector
t_1	horizontal wall thickness to chord ratio	L	lift
t_2	vertical wall thickness to chord ratio	NC	number of constraints
w_c	spar width to chord ratio	NDV	number of design variables
w_s	wing span	$NOBJ$	number of objective functions
		Q	flow variables
		R	discretized flow equations

This research was performed under a grant from NASA Ames Research Center, Grant Number, NCA2-778, Technical Monitor T. A. Edwards. The authors would like to extend their thanks to S. Cheung, NASA Ames Research Center, for his technical assistance and the National Center for Supercomputing Applications, University of Illinois at Urbana-Champaign, for providing additional computing time.

W	weight of the aircraft	max	maximum
X	vector of grid coordinates	n	quantities at a new point
ε	objective function tolerance	ref	reference
ϕ	design variable vector	SUPERSCRIPITS	
λ	leading edge sweep	L	lower limit
σ	wing root stress	T	transpose
SUBSCRIPTS		U	upper limit
all	allowable value	1, 2	level 1, 2
i	i^{th} quantity	*	steady state solution or optimum solution
min	minimum		

1. BACKGROUND

Analysis and design of aerospace vehicles are associated with complex multidisciplinary couplings. The development of an efficient optimization procedure for the design of aircraft must incorporate the interactions between disciplines such as aerodynamics, dynamics, aerolastic stability, structures, controls and acoustics. However, the validity of the designs obtained using optimization techniques depends strongly upon the accuracy of the analysis procedures used and it is essential to integrate sufficiently comprehensive analysis procedures within the closed-loop optimization. Such procedures are computationally intensive, and therefore, can be prohibitive within an optimization environment. For example, it is essential to use a comprehensive aerodynamic analysis procedure to solve the complex flow field associated with high speed aircraft. Over the past few years, Computational Fluid Dynamics (CFD) has evolved rapidly with the development of numerous numerical algorithms. Although accurate detailed analyses of many complex flow fields are now possible using supercomputers, viscous-compressible flow simulations of wing-body configurations can require several CPU hours per steady-state solution. Therefore, the use of such comprehensive analytical procedures for design optimization can be prohibitively expensive if a gradient-based technique is used.

Sensitivity analysis, in which the derivative of a system performance function (e.g., the lift or drag of an aircraft) with respect to a design variable (e.g., a parameter controlling the wing planform) is calculated, is an essential ingredient in design optimization. A widely used technique for performing aerodynamic sensitivity analysis is the method of finite differences. The use of this method is associated with several calls to the flow analysis routine. Although this technique is conceptually simple, the associated computational cost is prohibitive when used in an optimization problem involving a large number of design variables. Therefore, it is necessary to develop efficient techniques to calculate aerodynamic sensitivities, so that advanced CFD codes may be more useful as practical design tools in multidisciplinary optimization environments.

Two popular alternatives to the finite difference technique are the direct differentiation approach and the adjoint variable approach. These techniques are widely used in structural sensitivity calculations [1,2]. In both techniques, the actual governing equations are differentiated with respect to the design variables using the chain rule. The direct differentiation approach yields a large system of equations involving the desired sensitivities that can be solved directly. In the adjoint variable approach, adjoint variables are obtained as the solution to an adjoint problem. The adjoint variables are then used to calculate the sensitivities. These two techniques are equivalent and yield identical results for the sensitivities. More recently, there has been widespread interest in using these techniques for calculating aerodynamic sensitivities. Carlson and Elbanna [3] have used the direct differentiation technique to differentiate the discretized transonic small perturbation equations and obtain aerodynamic sensitivities. Baysal *et al.* [4,5] have performed discrete sensitivity analysis using the Euler equations. Taylor *et al.* [6] and Newman *et al.* [7] have developed a semi-analytical sensitivity analysis procedure for the thin-layer Navier-Stokes equations using an incremental strategy. Jameson *et al.* [8] have proposed a continuous sensitivity approach

using the adjoint variable method to calculate aerodynamic sensitivities. In the continuous sensitivity approach, the governing equations are differentiated prior to their discretization. The sensitivities are calculated using a numerical algorithm similar to the one used for obtaining the flow solution. Therefore, the continuous sensitivity approach needs to be modified, depending upon the governing equations that are differentiated. In the discrete sensitivity approach, the discretized governing algebraic equations are differentiated. Although there is a need for solving a large system of equations, this procedure can easily be adapted to different analysis procedures.

The necessity of multidisciplinary coupling in successful design optimization has been recognized. Recently, attempts have been made in coupling two or more of these disciplines, [9–13] in which optimization was performed by addressing all the design criteria in a single level. This “all-at-once” optimization procedure, in which all the disciplines are coupled inside a single loop and optimization is performed based on criteria involving every discipline, can be inefficient and time consuming. Decomposition techniques are often used to simplify such complex optimization problems into a number of sub-problems. Multilevel decomposition techniques have been applied to problems based on a single discipline [14–19] in structural applications. Recently, attempts have been made to use these techniques for multidisciplinary optimization of rotary wing aircraft. Adelman *et al.* [20] developed a two-level procedure for performing integrated aerodynamic, dynamic and structural optimization of rotor blades, based on the multilevel optimization strategy described in [17]. Chattopadhyay *et al.* [21] developed a three-level procedure for optimization of helicopter rotor blades with the integration of aerodynamics, dynamics, aeroelastic stability, and structures. In a multidisciplinary design problem, the number of levels in a multilevel decomposition procedure typically depends upon the number of disciplines involved. Individual optimization is performed at each level using analysis procedures pertaining to that level. Optimal sensitivity parameters are exchanged between the levels to provide the necessary coupling. An optimal design is obtained when each individual level is converged and overall convergence is achieved. Therefore, the speed of obtaining a fully converged result depends upon the strength of coupling between the various levels.

The objective of the present research is to develop an efficient multidisciplinary design optimization procedure which addresses the aerodynamic and structural design requirements of aerospace vehicles by using comprehensive analysis procedures and efficient sensitivity analysis technique. A semi-analytical sensitivity analysis technique, based on the direct differentiation approach, is developed to calculate the aerodynamic design sensitivities. The results from this technique are compared with those obtained using finite difference to establish its accuracy and efficiency. The technique is applied to the wing design of high speed aircraft. The procedure offers significant cost savings over the finite difference technique and allows for the use of comprehensive CFD codes within the closed-loop optimization.

2. PROBLEM FORMULATION USING MULTILEVEL DECOMPOSITION

This section describes the multilevel decomposition technique and the formulation of the aircraft design problem using this technique. The multilevel decomposition procedure is illustrated through a two-level formulation. Each level is a multiobjective optimization problem characterized by a vector of objective functions, constraints and design variables. During optimization at a particular level, it is essential to maintain the objective functions and design variables of lower levels close to their optimum values. Therefore, constraints are imposed on the perturbations to the lower level objective functions and design variables to prevent significant changes. These parameters are called optimal sensitivity derivatives, and they establish the necessary link between the various levels of optimization. The multilevel decomposition procedure is outlined below.

LEVEL 1.

$$\begin{aligned}
& \text{Minimize } F_i^1(\phi^1) && i = 1, \dots, NOBJ^1 \\
& \text{subject to } g_k^1(\phi^1) \leq 0 && k = 1, \dots, NC^1 \\
& \sum_{i=1}^{NDV^1} \frac{\partial F_j^{2*}}{\partial \phi_i^1} \Delta \phi_i^1 \leq \varepsilon_{2j} && j = 1, \dots, NOBJ^2 \\
& \phi_i^{1L} \leq \phi_i^1 \leq \phi_i^{1U} && i = 1, \dots, NDV^1 \\
& \phi_j^{2L} \leq \phi_j^{2*} + \sum_{i=1}^{NDV^1} \frac{\partial \phi_j^{2*}}{\partial \phi_i^1} \Delta \phi_i^1 \leq \phi_j^{2U} && j = 1, \dots, NDV^2
\end{aligned}$$

where F^1 and F^2 are the objective function vectors at levels 1 and 2 respectively, g^1 and g^2 are the corresponding constraint vectors and ϕ^1 and ϕ^2 are the corresponding design variable vectors. The quantity ε_{2j} is a tolerance on the change in the j^{th} objective of level 2 during optimization at level 1. Superscripts L and U represent lower and upper bounds respectively, and superscript $*$ represents optimum values obtained at level 2. Finally, the quantities, $\frac{\partial F_j^{2*}}{\partial \phi_i^1}$ and $\frac{\partial \phi_j^{2*}}{\partial \phi_i^1}$ are the optimal sensitivity parameters of level 2 objective function and design variable vectors, respectively, with respect to the level 1 design variables.

LEVEL 2.

$$\begin{aligned}
& \text{Minimize } F_i^2(\phi^{1*}, \phi^2) && i = 1 \dots NOBJ^2 \\
& \text{subject to } g_k^2(\phi^{1*}, \phi^2) \leq 0 && k = 1 \dots NC^2 \\
& \phi_i^{2L} \leq \phi_i^2 \leq \phi_i^{2U} && i = 1 \dots NDV^2
\end{aligned}$$

where ϕ^{1*} is the optimum design variable vector from level 1. This vector is kept fixed during optimization at level 2. The optimization procedure cycles through the two levels before global convergence is achieved. A ‘‘cycle’’ is defined as one complete sweep through the two levels of optimization. Optimization at an individual level also requires several ‘‘iterations’’ before local convergence is achieved. Cycling between the two levels is necessary to account for the coupling between the objective functions, constraints, and design variables pertaining to the levels.

The proposed decomposition of a wing-body optimization problem is described next. Since, in a typical aircraft design, the aerodynamic performance criteria primarily govern the planform of the wing, a hierarchical decomposition scheme is proposed in which the aircraft wing is optimized for improved aerodynamic performance at level 1 and improved structural performance at level 2.

In level 1, the drag coefficient of the aircraft, C_D , is the objective function which is minimized. Design variables, at this level, include the wing root chord, c_0 , the leading edge sweep, λ , the wing thickness to chord ratio, t_c , and the wing span, w_s (Figure 1). A constraint is imposed on the value of the lift coefficient ($C_L \geq C_{L_{\min}}$) to maintain the lift characteristics of the optimum wing above a minimum level. The value of $C_{L_{\min}}$ is chosen to be a certain percentage higher than the C_L of the reference wing. A constraint is also imposed on the level 2 objective function, the aircraft weight, W , (i.e., $W \leq W_{\text{ref}}$ where W_{ref} represents optimum weight as obtained from level 2) to ensure that improvement in aerodynamic performance does not incorporate weight penalty. It is to be noted that this is the coupling constraint illustrated in the two-level formulation with ε_{21} set to zero.

At level 2, the objective is to improve the structural performance of the aircraft without affecting its aerodynamic behavior. The aircraft weight is the objective function to be minimized. Constraints are imposed on stresses at the wing root section to ensure safe structural performance ($\sigma \leq \sigma_{\text{all}}$). Initially, to simplify the structural analysis, the load carrying structural member in

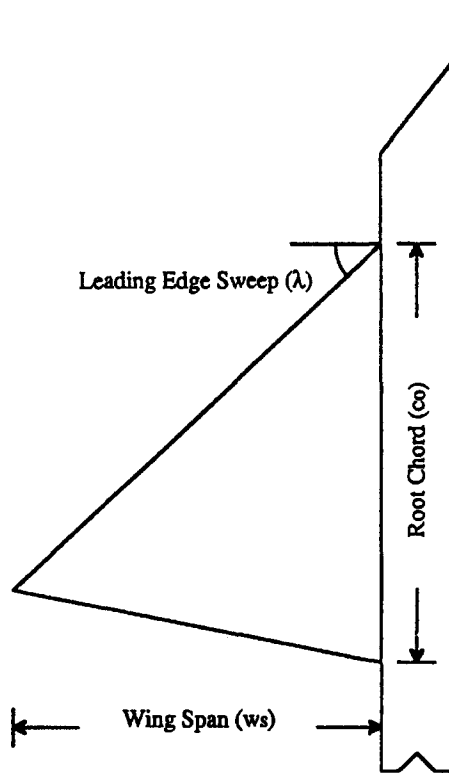


Figure 1. Airplane planform variables.

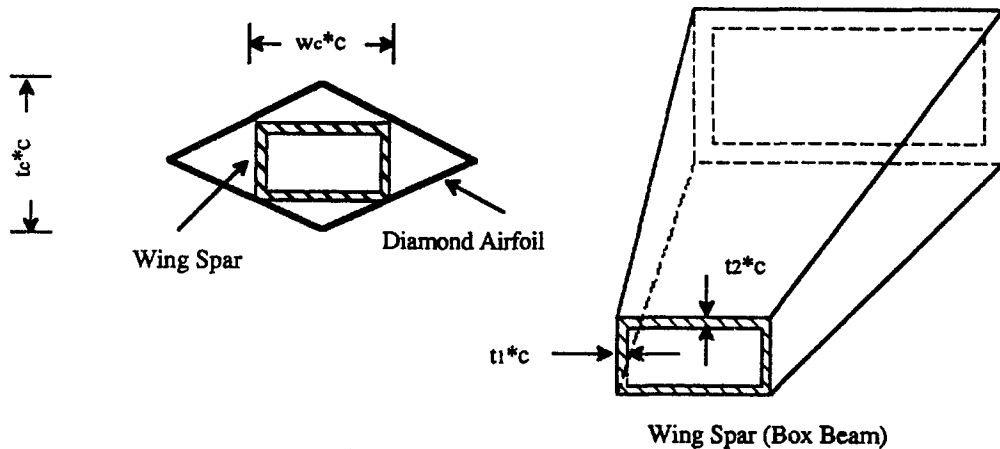


Figure 2. Wing cross-section and wing spar (box beam).

the wing is modeled as a single celled, isotropic box beam (Figure 2). The beam width to chord ratio, w_c , the horizontal wall thickness to chord ratio, t_1 , and the vertical wall thickness to chord ratio, t_2 , are used as design variables.

3. ANALYSIS

The parabolized Navier-Stokes equations (PNS equations) have been used for the evaluation of three-dimensional, supersonic, viscous flow fields. The PNS equations are obtained from the full Navier-Stokes equations based on the following assumptions:

- steady state,
- the streamwise viscous gradients are neglected, and
- the streamwise pressure gradient in the subsonic portion of the viscous flow near the body surface is approximated.

The inviscid region of the flow field must be supersonic and the streamwise velocity component must be positive everywhere. Thus, streamwise flow separation is not allowed but crossflow separation is allowed. Efficiency in computational time and memory requirements is achieved because the equations can be solved using a space-marching technique. The computational procedure used in this study, as implemented in the code, UPS3D [22], integrates the PNS equations using an implicit, approximately factored, finite-volume algorithm where the crossflow inviscid fluxes are evaluated by Roe's flux-difference splitting scheme [23]. The UPS3D code also has the capability to calculate the inviscid flow field by solving the PNS equations without the viscous terms. The upwind algorithm is used to improve the resolution of the shock waves over that obtained with the conventional central differencing schemes. A hyperbolic computational grid is used with 75 grid points along the circumferential direction, 40 grid points along the normal direction, and 31 grid points along the longitudinal direction. Figure 3 presents the surface grid for the wing body configuration. Further refinement of the grid does not change the flow solution significantly.

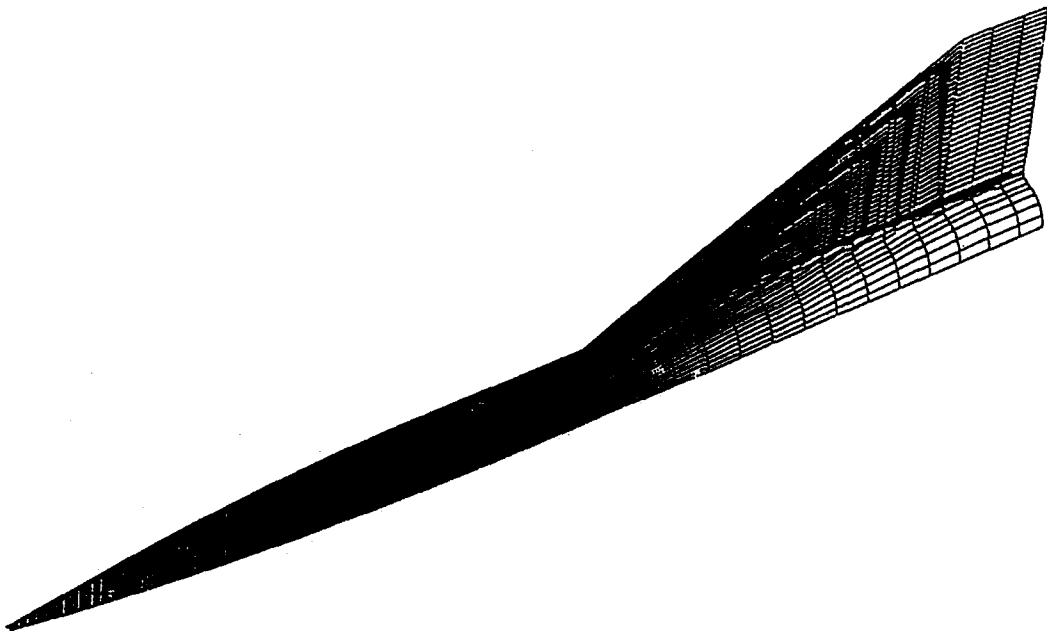


Figure 3. Surface grid of the wing-body configuration.

The aircraft wing structural analysis is performed using an inhouse code. The code is capable of analyzing multicelled box beams of arbitrary cross-section and tapered planform. The wing section is represented by a diamond airfoil (Figure 2). The principal load carrying member in the wing is modeled by an isotropic box beam with a rectangular cross-section and unequal wall thicknesses. The wall thicknesses are represented as fractions of local chord (c) as shown in Figure 2. The wing weight (W) is calculated as the sum of the weight of the box beam (W_{box}) and the weight of the skin (W_{skin}). The stresses (σ) are calculated using thin wall theory.

4. OPTIMIZATION AND SENSITIVITY ANALYSIS

A gradient based optimization technique based on the method of feasible directions [24] has been used to solve the optimization problems at levels 1 and 2. Structural sensitivity analysis is performed using exact analytical expressions. Aerodynamic sensitivity analysis is performed through direct differentiation of the discretized governing differential equations, which is briefly described below.

In general, an aerodynamic performance coefficient, C_j , depends on the steady-state flow variables, Q^* , the vector of computational grid coordinates, X , and, sometimes, explicitly on the vector of independent design variables, ϕ . Mathematically,

$$C_j = C_j(Q^*(\phi), X(\phi), \phi). \quad (1)$$

The derivative of C_j with respect to the i^{th} design variable, ϕ_i , is given by,

$$\left\{ \frac{dC_j}{d\phi_i} \right\} = \left\{ \frac{\partial C_j}{\partial Q^*} \right\}^\top \left\{ \frac{\partial Q^*}{\partial \phi_i} \right\} + \left\{ \frac{\partial C_j}{\partial X} \right\}^\top \left\{ \frac{\partial X}{\partial \phi_i} \right\} + \left\{ \frac{\partial C_j}{\partial \phi_i} \right\}. \quad (2)$$

In Equation 2, the terms $\left\{ \frac{\partial C_j}{\partial Q^*} \right\}$, $\left\{ \frac{\partial C_j}{\partial X} \right\}$ and $\left\{ \frac{\partial C_j}{\partial \phi_i} \right\}$ are easily calculated by knowing the explicit dependence of C_j on Q^* , X and ϕ_i . The term $\left\{ \frac{\partial X}{\partial \phi_i} \right\}$, called the grid sensitivity vector, can be calculated using any of the methods described in [25] and [26], or by using the finite difference technique. In this paper, the finite difference technique has been used to evaluate the grid sensitivity vector. The term $\left\{ \frac{\partial Q^*}{\partial \phi_i} \right\}$, which represents the sensitivity of the steady state flow variables with respect to the i^{th} design variable, is calculated using the direct differentiation technique described next.

The discretized PNS equations which model the flow can be written as

$$\{R(Q^*(\phi), X(\phi), \phi)\} = \{0\}. \quad (3)$$

Equation 3, differentiated with respect to ϕ_i , yields

$$\left\{ \frac{dR}{d\phi_i} \right\} = \left\{ \frac{\partial R}{\partial Q^*} \right\}^\top \left\{ \frac{\partial Q^*}{\partial \phi_i} \right\} + \left\{ \frac{\partial R}{\partial X} \right\}^\top \left\{ \frac{\partial X}{\partial \phi_i} \right\} + \left\{ \frac{\partial R}{\partial \phi_i} \right\} = \{0\}. \quad (4)$$

Equation 4 represents a set of linear algebraic equations which can be solved easily to obtain $\left\{ \frac{\partial Q^*}{\partial \phi_i} \right\}$. It is to be noted that the remaining terms in Equation 4, $\left\{ \frac{\partial R}{\partial Q^*} \right\}$, $\left\{ \frac{\partial R}{\partial X} \right\}$ and $\left\{ \frac{\partial R}{\partial \phi_i} \right\}$ are easy to calculate by knowing the explicit dependence of $\{R\}$ on Q^* , X and ϕ_i . Thus, all quantities in Equation 2 are calculated to yield the aerodynamic sensitivities, $\left\{ \frac{dC_j}{d\phi_i} \right\}$. The above technique is described in greater detail in [27].

Since the optimization process requires several evaluations of the objective function and the constraints before an optimum design is obtained, the process can be very expensive if actual analyses are performed for each function evaluation. The objective function and constraints at levels 1 and 2 are, therefore, approximated using a two-point exponential approximation [28] based on the design variable values from the optimizer and the sensitivities of these functions. The method has been found to provide good approximations in highly nonlinear constrained optimization problems [21]. Specifically, if a function F and its derivatives are calculated for the design ϕ_o , its value for a new design ϕ_n is given by

$$F(\phi_n) = F(\phi_o) + \sum_{i=1}^{NDV} \left(\left(\frac{\phi_{ni}}{\phi_{oi}} \right)^{p_i} - 1 \right) \frac{\phi_{oi}}{p_i} \frac{\partial F}{\partial \phi_i}(\phi_o) \quad (5)$$

where F is the function that is being approximated, ϕ_o is the old design variable vector and ϕ_n is the new design vector. The parameter p_i is used to control the approximation. For $p_i = 1$, the approximation reduces to a first order Taylor expansion. For $p_i = -1$, the approximation reduces to a reciprocal Taylor expansion. The parameter p_i is constrained to assume values between -1 and 1 . A move limit, typically defined as the maximum fractional change of each design variable value, is imposed as upper and lower bounds on each design variable ϕ_i to control the validity of the approximation.

5. RESULTS

Results, based on the semi-analytical sensitivity analysis procedure and the two level optimization procedure, are presented in this section. The procedures developed are applied to a reference wing-body configuration with root chord, $c_0 = 7.08$ m, leading edge sweep, $\lambda = 66.0$ degrees, wing span, $w_s = 2.96$ m, and wing thickness-to-chord ratio, $t_c = 0.052$. The cruise Mach number is set to 2.5 and the angle of attack is equal to 5.0 degrees. The load carrying structural member is modeled as an isotropic box beam made of 2014-T6 Aluminum alloy. The reference values of the spar width-to-chord ratio (w_c), spar horizontal wall thickness-to-chord ratio (t_1), and spar vertical wall-thickness-to chord ratio (t_2) are set equal to 0.5, 0.0015, and 0.0075 respectively. These values are based on the stiffnesses of a wing corresponding to a Mach 2.4 configuration.

The sensitivities of the drag coefficient (C_D) and the lift coefficient (C_L), calculated using the direct differentiation approach as well as the finite difference technique, are presented in Tables 1 and 2 respectively. It is seen that the results from both techniques are in good agreement. The computing time required to calculate the sensitivities using the finite difference technique is approximately 3000 CPU seconds per analysis whereas the direct differentiation technique only requires 2100 CPU seconds per analysis as shown in Figure 4. This demonstrates the efficiency of this technique (30 percent reduction in CPU time for each sensitivity analysis). The reduction in computing time is achieved because the finite difference technique requires $(NDV + 1)$ calls to the CFD code while the direct differentiation technique requires only one call for each sensitivity analysis. However, this reduction in CPU time is not dramatic because the direct differentiation technique requires the solutions of large linear systems of equations in the design sensitivities.

Table 1. Sensitivity of the drag coefficient, C_D .

Derivative w.r.t.	Finite Difference	Direct Differentiation
Sweep (λ)	-0.00700	-0.00756
Root Chord (c_0)	-0.00791	-0.00833
Wing Span (w_s)	0.78846	0.83009
Thickness-to-chord ratio (t_c)	0.00068	0.00071

Table 2. Sensitivity of the lift coefficient, C_L .

Derivative w.r.t.	Finite Difference	Direct Differentiation
Sweep (λ)	-0.05697	-0.05931
Root Chord (c_0)	0.01977	0.02036
Wing Span (w_s)	-0.23077	-0.24132
Thickness-to-chord ratio(t_c)	0.01351	0.01445

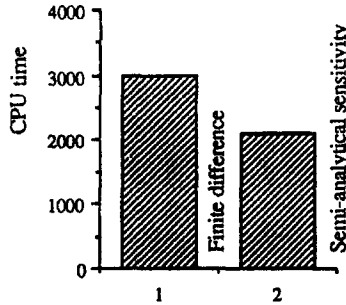


Figure 4. Comparison of CPU time consumed by semi-analytical and finite difference techniques.

During the level 1 aerodynamic optimization, the optimum results are obtained after an average of 5 iterations through the optimizer. During the level 2 structural optimization, the optimum

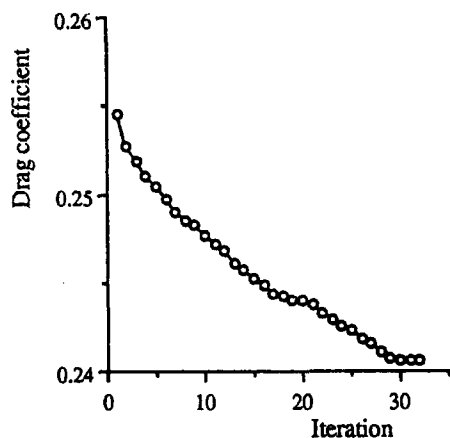


Figure 5. Iteration history of drag coefficient.

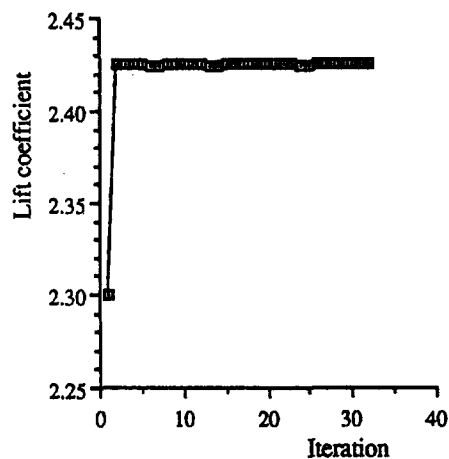


Figure 6. Iteration history of lift coefficient.

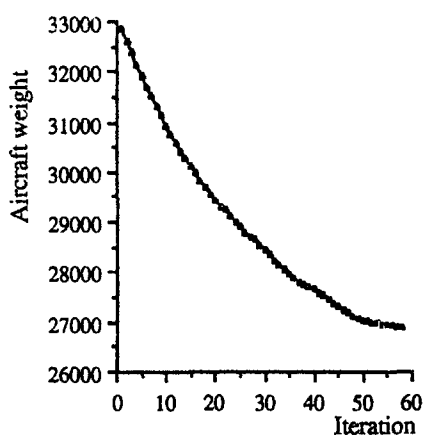


Figure 7. Iteration history of aircraft weight.

results are obtained after an average of 8 iterations through the optimizer. The two-level optimization converges after 7 complete cycles. In both levels, a move limit of 2 percent is used for the design variables.

The iteration histories of the drag coefficient and the lift coefficient of the aircraft during the level 1 aerodynamic optimization are presented in Figures 5 and 6 respectively. Significant improvements are observed in both the quantities. The drag coefficient decreases by 5.5 percent and the lift coefficient increases by 5.43 percent. It is to be noted that the drag and the lift coefficients are calculated based on a unit reference area and not based on the wing planform area. The lift coefficient is maintained at its improved value throughout the optimization procedure because, the lift coefficient constraint, imposed during the aerodynamic optimization, remains an active constraint. The optimizer, based on the method of feasible directions, remains on this constraint boundary, as it improves the objective function value. The constraint imposed on the aircraft weight, at level 1, is well satisfied during the level 1 optimization. The value of ε_{21} is chosen to be zero which indicates that the aircraft weight, during the level 1 aerodynamic optimization, is constrained to be lesser than or equal to its optimum value from the structural optimization. Table 3 compares the reference and the optimum values of the aerodynamic design variables used in the aerodynamic optimization. The root chord is increased significantly from its reference value (8.76 percent), whereas the wing thickness-to-chord ratio is decreased significantly (40.29 percent). The wing span and the leading edge sweep are maintained close to their reference values (2.94 percent and 1.01 percent respectively). The reduction in the wing thickness-to-chord ratio decreases the form drag of the diamond airfoil section. The optimization is driven by this reduction in drag. The increase in the wing planform area, caused by the increase in the root

Table 3. Aerodynamic design variables.

Design variable	Reference	Optimum
Sweep (λ)	66.00 deg.	65.33 deg.
Root Chord (c_o)	7.08 m	7.70 m
Wing Span (w_s)	2.96 m	3.047 m
Thickness-to-chord ratio (t_c)	0.05200	0.03105

Table 4. Structural design variables.

Design variable	Reference	Optimum
Spar width-to-chord ratio (w_c)	0.5	0.2
Horizontal wall thickness-to-chord ratio (t_1)	0.0015	0.0006
Vertical wall thickness-to-chord ratio (t_2)	0.0075	0.00261

chord and the wing span, helps improve the lift of the aircraft in spite of the decrease in the wing thickness-to-chord ratio.

The iteration history of the aircraft weight is presented in Figure 7. Considerable reduction (18.13 percent) in the aircraft weight is observed from the reference to the optimum. The shear and the normal stresses at the blade root remain well within the allowable limits of the chosen Aluminum alloy. Table 4 compares the reference and optimum values of the structural design variables used in the structural optimization. The optimum spar width to chord ratio, horizontal and vertical wall thickness to chord ratios decrease significantly from their reference values (60 percent, 60 percent and 65.2 percent respectively). As mentioned above, the optimum configuration has an increased planform area compared to the reference configuration. It must be noted that the optimum weight is still lower than the reference due to the significant reduction in the wall thicknesses.

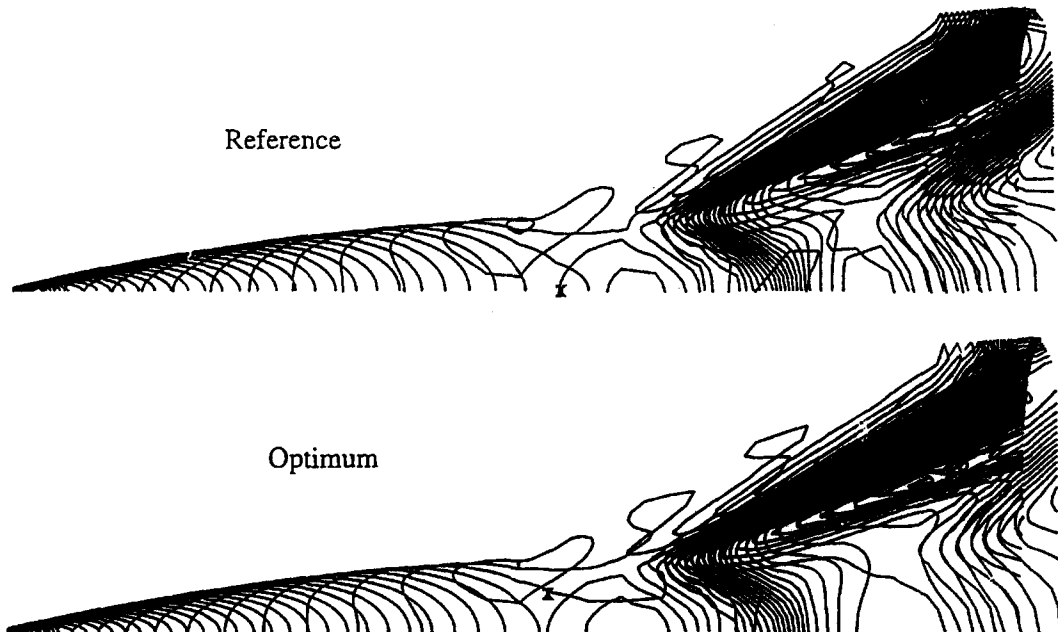


Figure 8. Surface pressure contours for reference and optimum configurations.

It is important to ensure that the optimization procedure does not deteriorate the flow behavior past the wing-body configuration and the solution does not have any abnormalities. Figure 8 presents the surface pressure contours for the reference and the optimum configurations. It

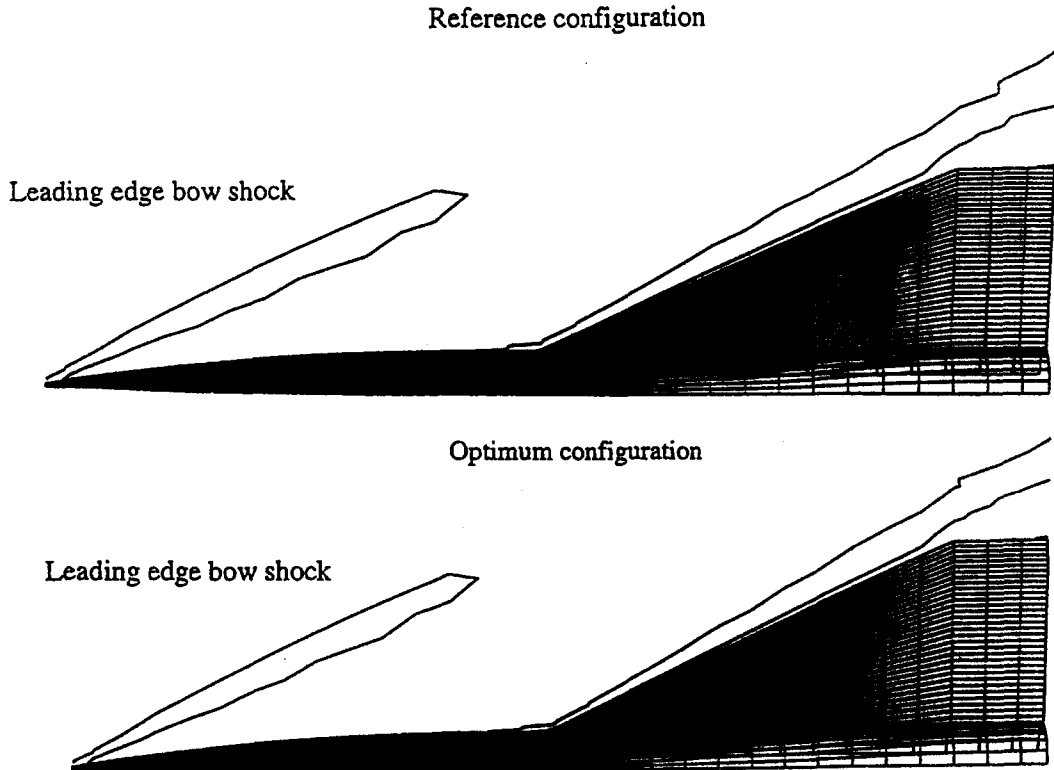


Figure 9. Leading edge shock shapes for reference and optimum configurations.

is clear from these contour plots that the flow solutions for the reference and the optimum configurations show similar trends and do not have abnormalities. Further, if the leading bow shock interferes with the wing, it causes significant deterioration in the aerodynamic performance. Figure 9 presents the bow shocks for the reference and the optimum wing-body configurations. As shown, the bow shocks do not interfere the wing in either case, ascertaining that the optimization procedure yields configurations with normal flow behavior.

6. CONCLUDING REMARKS

An efficient, semi-analytical sensitivity analysis technique, based on the direct-differentiation approach, and a multidisciplinary, multilevel based optimization procedure have been developed. The aircraft aerodynamic and structural design requirements have been coupled within a two-level optimization procedure. The following observations are made.

1. The direct differentiation technique developed offers significant cost reduction over the finite difference technique (30 percent per sensitivity analysis) and allows for the use of comprehensive analysis procedures within the closed loop optimization.
2. The multilevel decomposition optimization procedure yields significant reduction in the aircraft drag and weight while improving the lift.
3. The reduction in the aircraft drag is predominantly due to the significant reduction in the wing thickness-to-chord ratio. The improvement in the lift is due to the increased planform area caused by the increases in the wing root chord and wing span.

REFERENCES

1. J.J. Tsay and J.S. Arora, Nonlinear structural design sensitivity analysis for path dependent problems. Part 1: General theory, *Computer Methods in Applied Mechanics and Engineering* **81**, 183-208, (1990).
2. A. Chattopadhyay and R. Guo, Nonlinear structural design sensitivity analysis for composites undergoing elastoplastic deformation, *Composites Engineering*, (1993) (to appear).

3. H. Elbanna and L. Carlson, Determination of aerodynamic sensitivity coefficients in the transonic and supersonic regimes, *27th Aerospace Sciences Meeting*, AIAA Paper No. 89-0532, Reno, NV, (1989).
4. O. Baysal and M.E. Elashaky, Aerodynamic sensitivity analysis methods for the compressible Euler equations, *Journal of Fluids Engineering* **113** (4), 681–688, (1991).
5. G.W. Burgreen and O. Baysal, Three-dimensional aerodynamic shape optimization of wings using sensitivity analysis, *32nd Aerospace Sciences Meeting*, AIAA Paper No. 94-0094, Reno, NV, (1994).
6. V.M. Korivi, A.C. Taylor, P.A. Newman, G.J.W. Hou and H.E. Jones, An approximately factored incremental strategy for calculating consistent discrete aerodynamic sensitivity derivatives, *AIAA-92-4746-CP*.
7. P.A. Newman, G.J.W. Hou, H.E. Jones, A.C. Taylor and V.M. Korivi, Observations on computational methodologies for use in large-scale, gradient-based, multidisciplinary design, *AIAA-92-4753-CP*.
8. J. Reuther and A. Jameson, Control theory based airfoil design for potential flow and a finite volume discretization, *32nd Aerospace Sciences Meeting*, AIAA Paper No. 94-0499, Reno, NV, (1994).
9. J. Sobieszcanski-Sobieski, Sensitivity analysis and multidisciplinary optimization for aircraft design: Recent advances and results, *NASA TM100630*, (1988).
10. J.F.M. Barthelemy, G.A. Wrenn, A.R. Dovi and P.C. Coen, Integrating aerodynamics and structures in the minimum weight design of a supersonic transport wing, *33rd AIAA/ASME/AHS/ASCE Structures, Structural Dynamics and Materials Conference*, Dallas, TX, (1992).
11. J.F.M. Barthelemy, P.G. Coen, G.A. Wrenn, M.F. Riley, A.R. Dovi and L.E. Hall, Application of multidisciplinary optimization methods to the design of a supersonic transport, *NASA TM-104073*.
12. A. Chattopadhyay, J.L. Walsh and M.F. Riley, Integrated aerodynamic/dynamic optimization of helicopter blades, *Special Issue of the AIAA Journal of Aircraft on Multidisciplinary Optimization of Aeronautical Systems II*, 58–64, (1991).
13. H.M. Adelman, J.L. Walsh and J.I. Pritchard, Recent advances in multidisciplinary optimization of rotorcraft, *NASA TM 107665*, (1992).
14. L.A. Schmit and M. Merhinfar, Multilevel optimum design of structures with fiber-composite stiffened-panel components, *AIAA Journal* **20** (1), 138–147, (1982).
15. L.A. Schmit and K.J. Chang, A multilevel method for structural synthesis, *25th AIAA/ASME/AHS/ASCE Structures, Structural Dynamics and Materials Conference*, Palm Springs, CA, (1984).
16. U. Kirsch, An improved multilevel structural synthesis method, *Journal of Structural Mechanics* **13** (2), 123–144, (1985).
17. J. Sobieszcanski-Sobieski, B.B. James and M.F. Riley, Structural optimization by generalized, multilevel optimization, *26th AIAA/ASME/AHS/ASCE Structures, Structural Dynamics and Materials Conference*, Orlando, FL, (1985).
18. Barthelemy, J.F.M. and Riley, M.F., Improved multilevel optimization approach for the design of complex engineering systems, *AIAA Journal* **26** (3), 353–360, (1988).
19. C.L. Bloebaum and P. Hajela, Heuristic decomposition for nonhierarchical systems, *32nd AIAA/ASME/AHS/ASCE Structures, Structural Dynamics and Materials Conference*, AIAA Paper 91-1039, Baltimore, MD, (1991).
20. H.M. Adelman, J.L. Walsh and J.I. Pritchard, Recent advances in integrated multidisciplinary optimization of rotorcraft, *4th AIAA/USAF/NASA/OAI Symposium on Multidisciplinary Analysis and Optimization*, AIAA Paper 92-4777-CP, Cleveland, OH, (1992).
21. A. Chattopadhyay, T.R. McCarthy and N. Pagaldipti, A multilevel decomposition procedure for efficient design optimization of helicopter rotor blades, *19th European Rotorcraft Forum*, Paper No. G7, Italy, (1993).
22. S.L. Lawrence, D.S. Chaussee and J.C. Tannehill, Application of an upwind algorithm to the three-dimensional parabolized Navier Stokes equations, *AIAA 8th Computational Fluid Dynamics Conference*, Honolulu, HI, (1987).
23. P.L. Roe, Approximate Reimann solver, parameter vectors and difference schemes, *Journal of Computational Physics* **43**, 357–372, (1981).
24. G.N. Vanderplaats, CONMIN-A FORTRAN program for constrained function minimization, Users' Manual, NASA TMX-62282, (1973).
25. A.C. Taylor, G.J.W. Hou and V.M. Korivi, Sensitivity analysis, approximate analysis and design optimization for internal and external viscous flows, AIAA Paper 91-3083, (September, 1991).
26. I. Sadrehaghghi, and R.E. Smith, Jr., and S.N. Tiwari, An analytical approach to grid sensitivity analysis, AIAA Paper 92-0660, (January, 1992).
27. A. Chattopadhyay and N. Pagaldipti, A discrete semi-analytical procedure for aerodynamic sensitivity analysis including grid sensitivity, *5th AIAA/NASA/USAF/ISSMO Symposium on Multidisciplinary Analysis and Optimization*, Panama City, FL, (September, 1994).
28. G.M. Fadel, M.F. Riley, and J.F.M. Barthelemy, Two-point exponential approximation method for structural optimization, *Structural Optimization* **2**, 117–124, (1990).